EEPO3

LPSC Grenoble, France, October 14-17, 2003

# Probing nucleon-nucleon correlations with $(\mathrm{e}, \mathrm{e}'\mathrm{p})$ and $(\mathrm{e}, \mathrm{e}'\mathrm{pp})$ reactions

J. Ryckebusch

*Department of Subatomic and Radiation Physics, Ghent University, Belgium*
*http://inwpent5.UGent.be/*

**Abstract**

Some of the recent attempts to detect signals of nucleon-nucleon correlations with semi-exclusive $A(e, e'p)$ and exclusive $A(e, e'pN)$ processes are reviewed. Unfactorized and distorted-wave calculations for these processes are discussed. The calculations implement two-body currents stemming from pion-exchange and intermediate $\Delta$ excitation. The two-body currents are shown to be highly competitive with the mechanisms related to nucleon-nucleon correlations. This observation seriously hampers attempts to link semi-exclusive $A(e, e'p)$ measurements, which probe high missing energies, to the correlated part of the nuclear spectral function. Signals of central short-range correlations (SRC) have been detected in $(e, e'pp)$ measurements on $^{12}$C and $^{16}$O, thereby confirming the picture that in hadronic matter SRC solely affect nucleon pairs with a small center-of-mass momentum and residing in a relative $S$ state.

## 1 Introduction

Two types of reactions involving electrons have been advocated as potentially powerful tools to learn about that part of the nuclear dynamics which cannot be understood as a mean-field phenomenon. First, semi-exclusive $A(e, e'p)$ reactions, which probe the continuous part of the spectral function, allow to study high-momentum protons in kinematic conditions which favor the occurrence of highly correlated nucleon pairs. In interpreting the data, however, great care must be exercised in evaluating the effect of competing processes, like final-state re-scatterings, pion-production through intermediate $\Delta$ creation and two-body meson-exchange currents. Second, triple-coincidence $A(e, e'pp)$ and $A(e, e'pn)$ measurements are challenging and gained momentum from 1990 on-wards. Measurements of two-proton knockout cross sections on the target nuclei $^3$He [1,2], $^{12}$C [3] and $^{16}$O [4,5] performed at Mainz, Amsterdam and Jefferson Lab, indicated important contributions from intermediate $\Delta$ creation. Information about the short-range correlations (SRC) can be extracted by comparing model calculations to the data. These comparisons provided evidence that only

diprotons residing in a relative $S$ state and having a small center-of-mass (C.M.) momentum, are subject to SRC. The wave function describing the C.M. motion of diprotons, on the other hand, was found to be completely in line with mean-field predictions up to momenta of 0.5 GeV [3,6]. To date, attempts to measure $A(e, e'pn)$ cross sections aim at providing information about tensor correlations in nuclei.

This contribution is organized as follows. In Sect. 2 the use of correlation functions to implement nucleon-nucleon correlations in reaction-model calculations will be sketched. Sect. 3 outlines a method of extracting information about the correlation functions from measured two-nucleon knockout data. Sect. 4 introduces an unfactorized model for computing $A(e, e'p)$ cross sections at missing energies above the two-nucleon emission threshold.

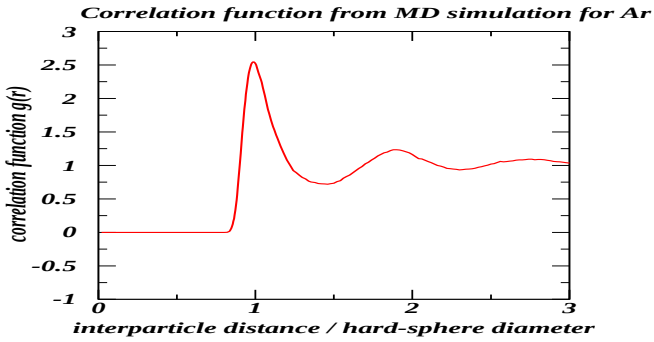


Figure 1: Typical correlation function from a molecular-dynamics (MD) simulation of hard spheres interacting through a Van Der Waals interaction.

## 2 Correlations and electro-induced hadron knockout

An efficient way of modeling the "fluctuations" (or, beyond mean-field behavior) of interacting many-body systems are the correlation functions which in their simplest form are defined as

$$G(r_1, r_2) = \langle r_1\ r_2 \rangle - \langle r_1 \rangle \langle r_2 \rangle \ . \tag{1}$$

In most interacting quantum systems, the correlation function depends solely on the relative coordinate $r_{12} =\mid \vec{r}_1 - \vec{r}_2 \mid$. In nuclear systems the correlation functions are effectively operators due to the state dependence of the nucleon-nucleon force. The major fraction of the correlations in hadronic matter can be incorporated economically by means of a correlated wave function of the type [7]

$$\left|\widetilde{\Psi}\right\rangle \equiv \frac{\widehat{\mathcal{G}}\left|\Phi\right\rangle}{\left\langle \Phi \left| \widehat{\mathcal{G}}^\dagger \widehat{\mathcal{G}} \right| \Phi \right\rangle} \ , \tag{2}$$

where $\Phi$ is a Slater determinant. The correlation operator has a spin, isospin and tensor dependence

$$\widehat{\mathcal{G}} = \widehat{\mathcal{S}} \left[ \prod_{i<j=1}^{A} \left( 1 - g_c(r_{ij}) + f_{t\tau}(r_{ij}) \widehat{S_{ij}} \vec{\tau}_i . \vec{\tau}_j + f_{\sigma\tau}(r_{ij}) \vec{\sigma}_i \vec{\sigma}_j \vec{\tau}_i . \vec{\tau}_j \right) \right] ,$$

where $\widehat{\mathcal{S}}$ is the symmetrizing operator. The short-range correlations (SRC) are usually associated with the so-called "central" correlation function $g_c(\mid \vec{r}_1 - \vec{r}_2 \mid)$ and can be linked with the finite extension of the nucleons which gives rise to a strong repulsion at short inter-nucleon distances. In many respects, the central correlation function for nucleons in nuclei can be expected to resemble those of molecules in liquids. As illustrated in Fig. 1, the latter exhibit a fluctuating behavior as a function of the intermolecular distance. Similarly, when moving with a nucleon in the nucleus, its finite extension will induce a reduced probability of finding another nucleon over distances of the order of its radius $R_p$ and an enhanced one at distances slightly larger than $R_p$. The limited spatial extension of a nucleus makes the fluctuating behavior of $g_c(r_{12})$ to fade out at inter-nucleon distances $r_{12}$ of a few femtometers.

Experimentally determining the correlation functions for nuclei turns out to be challenging. SRC effects are notoriously difficult to chase with the electromagnetic probe [8]. Indeed, the continuity equation

$$\vec{\nabla}_{\vec{r}} \cdot \vec{J}(\vec{r}) + \frac{1}{i\hbar} \left[ \rho(\vec{r}), \hat{H} \right] = 0 \;\; \text{with,} \;\; \hat{V}(1,2) = f(r_{12}) \vec{\sigma}_1 \cdot \vec{\sigma}_2 \;\; \vec{\tau}_1 \cdot \vec{\tau}_2 \, , \qquad (3)$$

demands that the corresponding $\vec{J}^{[2]}$ obeys

$$\vec{\nabla} \cdot \vec{J}^{[2]}(\vec{r}_1, \vec{r}_2; \vec{r}) = - \mid e \mid \;\; f(r_{12}) \vec{\sigma}_1 \cdot \vec{\sigma}_2 \times \left[ \delta(\vec{r} - \vec{r}_1) - \delta(\vec{r} - \vec{r}_2) \right] (\vec{\tau}_1 \times \vec{\tau}_2)_z \, . \qquad (4)$$

At short ranges one has that $\vec{r}_1 \longrightarrow \vec{r}_2$ and $\vec{\nabla} \cdot \vec{J}^{[2]} \approx 0$. Accordingly, exchange currents are dominated by the "longer-range" pion exchanges and "short-range" phenomena tend to hide themselves for the electromagnetic probe.

## 3 SRC and $A(e, e'NN)$ reactions

The link between SRC and the two-nucleon knockout $A(e, e'NN)$ cross sections can be easiest seen in the so-called factorized approach. In the spectator approximation this limit can be reached by describing the emerging nucleons in terms of plane-waves and assuming that the reaction occurs at short relative distances $\mid \vec{r}_{12} \mid \approx 0$. Then, the cross section takes on the formal form

$$\frac{d^8\sigma}{d\epsilon' d\Omega_{\epsilon'} d\Omega_1 d\Omega_2 dT_{p_2}}(e, e' N_1 N_2) = E_1 p_1 E_2 p_2 f_{rec}^{-1} \sigma_{eN_1N_2}(k_+, k_-, q) F_{h_1,h_2}(P) \, , \qquad (5)$$

where the relative momentum $\vec{p}_{rel}$ and C.M. momentum $\vec{P}$ of the pair is

$$\vec{p}_{rel} = \vec{k}_{\pm} = \frac{\vec{p}_1 - \vec{p}_2}{2} \pm \frac{\vec{q}}{2} \qquad \vec{P} = \vec{p}_1 + \vec{p}_2 - \vec{q}\,. \tag{6}$$

In these expressions, $\vec{p}_1$ and $\vec{p}_2$ are the measured momenta of the ejectiles. In a naive spectator approach, the quantity $P$ corresponds with the C.M. momentum of the diproton at the moment that it is hit by the virtual photon. In an ideal world with vanishing FSI mechanisms, $p_{rel}$ denotes the two possible values for the relative momentum of the bound pair. Further, $F_{h_1,h_2}(P)$ is the combined probability to find a dinucleon with C.M. momentum $P$ in the quantum state defined by two single-particle levels $(h_1, h_2)$ and $\sigma_{eN_1N_2}\,(k_+, k_-, q)$ is the probability to have an electromagnetic interaction with a dinucleon with relative momentum $k_{\pm}$. For the $A(e, e'pp)$ case, an analytical expression for $\sigma_{eN_1N_2}\,(k_+, k_-, q)$ has been derived [9]. It accounts for two-body effects induced by $\Delta$ currents, central, tensor and spin-isospin correlations. The function $\sigma_{eN_1N_2}$ plays an analogous role as the off-shell electron-proton $\sigma_{ep}^{(CCx)}$ functions in $A(e, e'p)$.

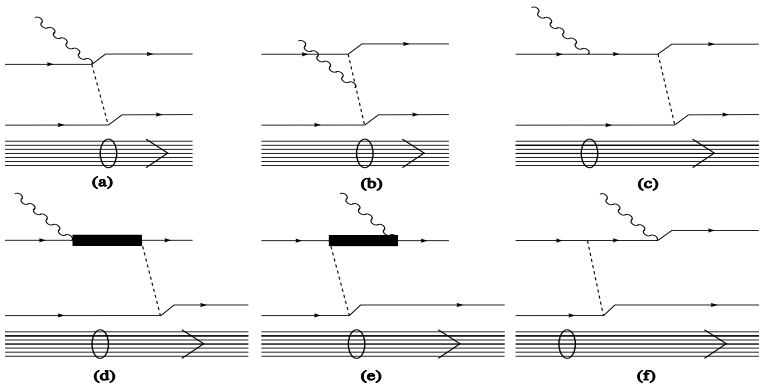


Figure 2: Typical diagrams included in a spectator model for electromagnetically induced two-nucleon knockout . Diagrams (a) and (b) are meson-exchange contributions. Further, (c) and (f) represent the initial- and final-state correlations. The $s$- and $u$-channel contribution for intermediate $\Delta$ creation and subsequent decay are (d) and (e).

Various unfactorized microscopic models for computing $\mathrm{A}(e, e'NN)$ ($\mathrm{A} \geq 12$) observables have been developed over the last number of years [10,11,12]. They all adopt the spectator approximation and a distorted-wave description for the emerging nucleons. Furthermore, differential cross sections can be computed for each of the individual states in the final nucleus. All models include intermediate $\Delta$ excitation and SRC effects, but differ in the way these mechanisms are implemented. A summary of the diagrams which are usually implemented is displayed in Fig. 2.

The first high-resolution $A(e, e'pp)$ data which could clearly separate the individual states in the final nucleus became recently available [5,13]. The data were collected by the A1 collaboration with a unique three-spectrometer setup

at the MAMI facility in Mainz. An initial electron beam energy of 855 MeV and an $^{16}$O target was used. The two ejected protons, with momenta $\vec{p}_1$ and $\vec{p}_2$, were detected parallel and anti-parallel to the momentum transfer, a peculiar situation which is known as "super-parallel kinematics". The energy and momentum transfer was $<\omega>$=215 MeV and $<q>$=316 MeV. Data were collected in a pair C.M. momentum range of $-100 \leq P \leq 400$ MeV/c.

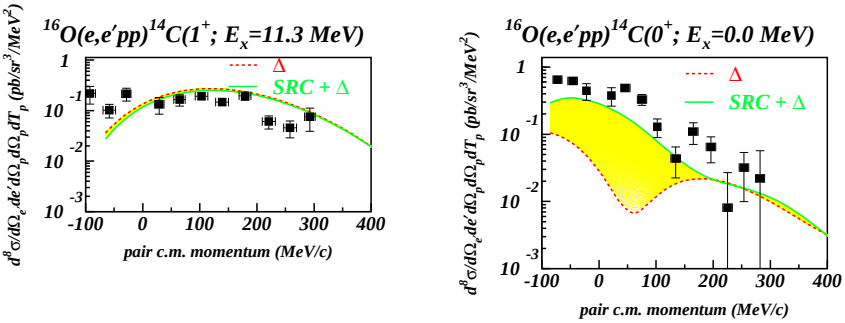


Figure 3: The eightfold differential cross section for the $^{16}\mathrm{O}(e,e'pp)^{14}\mathrm{C}(0^+, E_x = 0\ MeV)$ and the $^{16}\mathrm{O}(e,e'pp)^{14}\mathrm{C}(1^+, E_x = 11.31\ MeV)$ reaction as a function of the pair C.M. momentum. The (red) dashed curve shows the results of the distorted-wave calculations implementing only intermediate $\Delta$ excitation. The (green) solid curve is the result of a distorted-wave calculation that accounts for both intermediate $\Delta$ and central short-range correlations. The data are from Refs. [5] and [13].

Figure 3 presents a comparison between the Mainz $^{16}\mathrm{O}(e,e'pp)$ data of Ref. [5] and our distorted-wave calculations for two specific states in the residual nucleus. More results can be found in Ref. [14]. We start our discussion with the $1^+$ state at an excitation energy of $E_x$ =11.31 MeV in the residual nucleus $^{14}$C. In most nuclear-structure calculations, the two-proton overlap amplitudes for this particular state are dominated by the $\left|\left(1p_{3/2}\right)^{-1}\left(1p_{1/2}\right)^{-1};1^+\right\rangle$ two-hole configuration. The Moshinsky transformation serves as a guide to identify the dominant relative and C.M. quantum numbers of the diprotons for a specific transition. Indeed, the quantum numbers of the final state impose strong restrictions on the possible combinations for the relative and C.M. angular momentum of the active diproton. For the $\left|(1p)^{-2};1^+\right\rangle$ configuration only the combination of $L = 1$ C.M. and $P$-wave relative wave functions for the diproton is allowed. A striking feature of the calculations for the $1^+$ state displayed in Fig. 3 is that the intermediate $\Delta$ diagrams prevail in the computed angular cross sections, while SRC effects are marginal. Figure 3 displays also a comparison of the $^{16}\mathrm{O}(e,e'pp)^{14}\mathrm{C}(0^+, E_x = 0\ MeV)$ data and our reaction model calculations. For the ground-state transition, the distorted-wave calculations including short-range correlations reproduce the C.M.-momentum dependence well, while underestimating the data by roughly a factor of two over the whole momentum range. An interesting observation from Fig. 3 is that the calculation ignoring

SRC effects, underestimates the data for the ground-state transition at low pair C.M. momenta by several factors. At high pair C.M. momenta the $L = 1$ C.M. wave dominates and the calculations neglecting SRC move closer to the data. In any case, without inclusion of central short-range correlations, neither the shape nor the magnitude of the data for the ground-state transition can be reproduced. We interpret this as strong evidence for short-range correlations for proton pairs residing in relative $^1S_0$ states. At the same time, and equally important, central short-range correlations appear to affect exclusively proton pairs residing in a relative $S$ state and having a small C.M. momentum. This corresponds with the picture that short-range correlations exclusively affect nucleon pairs when they reside close to each other, thereby making them to move with equal momentum in a back-to-back situation.

## 4 SRC and semi-exclusive $A(e, e'p)$ reactions

Often, the semi-exclusive $A(e, e'p)$ measurements [15] which probe high missing energies ($E_m$) and momenta ($p_m$) are interpreted starting from the following FACTORIZED expression

$$\frac{d^6\sigma}{dT_p d\Omega_p d\epsilon' d\Omega_{\epsilon'}}(e, e'p) = \frac{p_p E_p}{(2\pi)^3}\sigma_{ep}^{CC1} P\left(\vec{p}_m, E_m\right) \ , \tag{7}$$

which assumes a direct connection between the correlated part of the spectral function $P\left(\vec{p}, E\right)$ and the measured differential cross sections. The above expression which connects the measured differential cross section to the spectral function relies on the assumption that single-nucleon currents prevail and that the strength attributed to contaminating mechanisms like two-nucleon currents and re-scattering effects is highly suppressed. The two-nucleon knockout investigations reported in previous section, however, nicely illustrated the importance of two-nucleon meson-exchange (MEC) and isobar currents (IC) when chasing nucleon-nucleon correlations in nuclei. In Ref. [16] an UNFACTORIZED framework for computing semi-exclusive $A(e, e'p)$ cross sections is proposed. It postulates that single-nucleon knockout to the energy continuum in the (A-1) nucleus is a two-nucleon emission process whereby one of the emerging nucleons remains undetected. Relying on the model which was developed for two-nucleon knockout, the angular cross sections are determined through the following expression

$$\frac{d^6\sigma}{dT_p d\Omega_p d\epsilon' d\Omega_{\epsilon'}}(e, e'p) = \sum_{N\equiv p,n}\int d\Omega_N dE_{A-2}\frac{d^9\sigma}{dT_N d\Omega_N dT_p d\Omega_p d\epsilon' d\Omega_{\epsilon'}}(e, e'pN) \ , \tag{8}$$

which involves an integration over the phase space of the undetected nucleon. Our approach allows to compute the strength from the MEC and IC in the same framework in which also the contributions from ground-state correlations are determined. At the same time, it provides a unified description to $A(e, e'p)$ in the continuous part of the spectrum and $A(e, e'NN)$, the two most popular reactions used to detect signatures of nucleon-nucleon correlations.

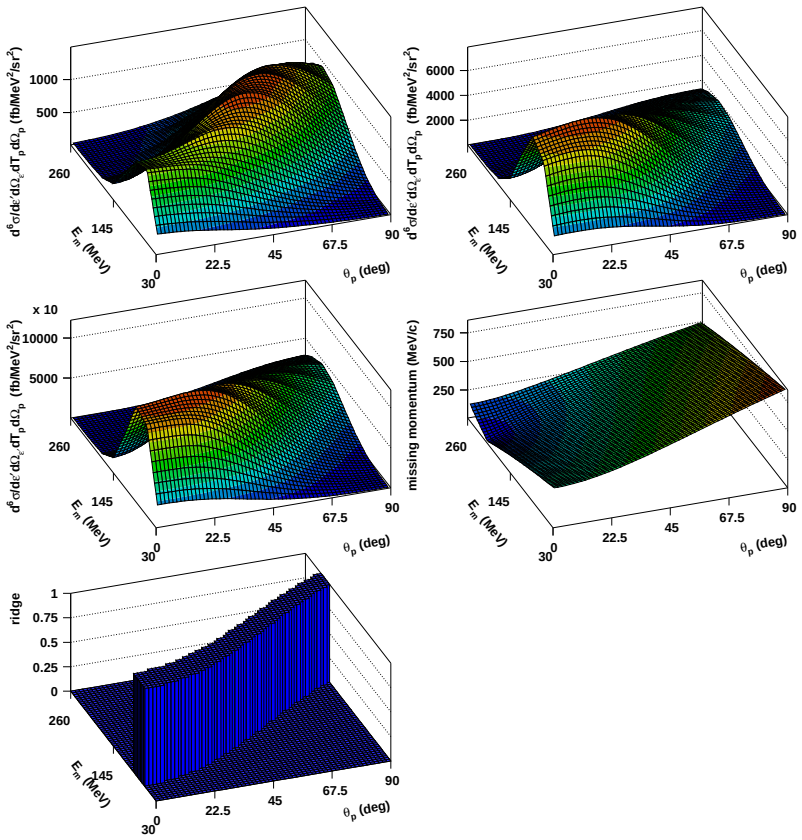


Figure 4: The differential $^{16}$O$(e,e'p)$ cross section versus missing energy ($E_m$) and proton angle ($\theta_p$) at $\epsilon$=1.2 GeV, $\epsilon'$=0.9 GeV and $\theta_e$=16$^o$ (or, $x \approx 0.15$ and $q = 0.42$ GeV/c). The upper left panel includes solely the central correlations and the upper right panel has both central and tensor correlations. The middle left panel includes apart from the central and tensor correlations also the MEC and IC. The variation of $p_m$ versus missing energy and proton angle is shown in the middle right panel. The lower left panel shows the position of the "ridge" (Eq. 9) in the $(E_m, \theta_p)$ plane. Hereby, the variable $< E_x^{h'} >$ was varied between 0. and 40. MeV.

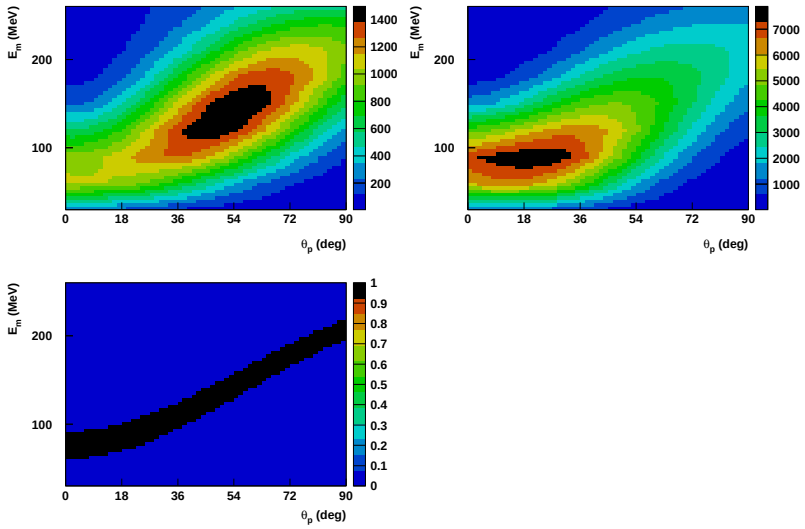


Figure 5: Contour plots corresponding with the upper and lower panels of Fig. 4.

The $^{16}\mathrm{O}(e,e'p)$ differential cross sections presented in Fig. 4 correspond with a small Bjorken scaling variable $x \approx 0.15$ and are obtained by incoherently adding the separately computed $^{16}\mathrm{O}(e,e'pn)$ and $^{16}\mathrm{O}(e,e'pp)$ strengths. Thereby, two-nucleon knockout from all $(1s_{1/2}, 1p_{3/2}, 1p_{1/2})$ shell-combinations is included. We first address the issue how the central, tensor and spin-isospin correlations manifest themselves in the $(e,e'p)$ differential cross sections at high $E_m$. We display the differential $^{16}\mathrm{O}(e,e'p)$ cross section versus missing energy and polar angle (measured with respect to the direction of the momentum transfer). The variation with $\theta_p$ allows to study the $p_m$ dependence of the cross section at a fixed $E_m$. For the sake of convenience, a panel with the variation of $p_m$ versus $E_m$ and $\theta_p$ was added. Roughly speaking, the probed missing momentum $p_m$ increases with increasing $\theta_p$. Comparing the two upper panels in Fig. 4 it emerges that the strength attributed to the tensor correlations largely overshoots the strength from the central correlations. In particular, this holds for the small proton angles $\theta_p$. At these angles, typically the smallest missing momenta are probed. The effect of the spin-isospin correlations is at the few percent level. The central correlations are observed to manifest themselves in a wider range of the $(E_m, \theta_p)$ plane than the tensor correlations do. Apparently, the effect of the tensor correlations is confined to a region of relatively low and moderate missing momenta, whereas the contribution from the central correlations extends to higher proton angles $\theta_p$ where typically higher missing momenta are probed. This qualitative behavior of the calculated differential cross sections reflects the fact that central correlations are the most important correlations in the spectral function at really high missing momenta, whereas the intermediate range is

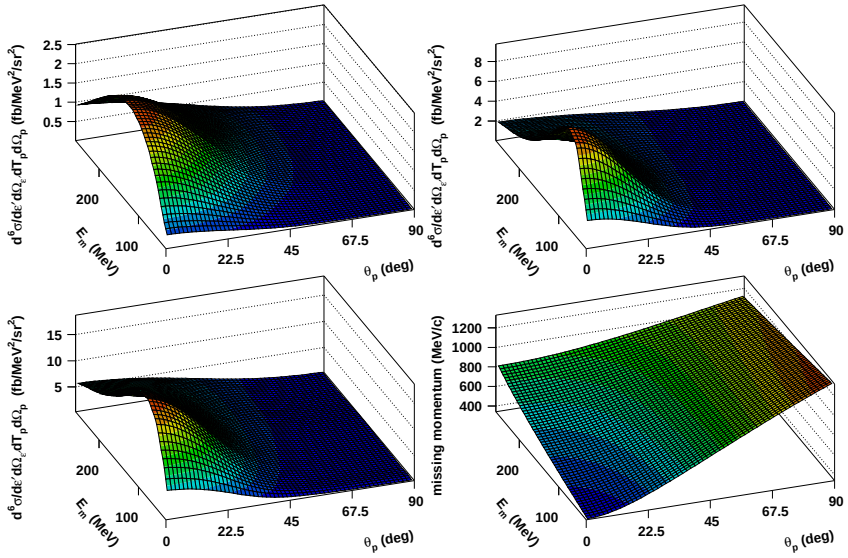


Figure 6: As in Fig. 4 but now for kinematics corresponding with Bjorken x $\approx$ 2, $\epsilon$=2.5 GeV and $Q^2$=1.1 GeV$^2$.

usually dominated by the tensor correlations.

Another interesting feature of how the ground-state correlations manifest themselves in the $(E_m, \theta_p)$ plane is that the peak of the $^{16}$O$(e, e'p)$ differential cross sections shifts to higher missing energies $E_m$ as one gradually moves to non-parallel kinematics and higher $p_m$ values are probed. This observation is a manifestation of a well-known feature of the correlated part of the spectral function, namely that the average missing energy $\langle E_m \rangle$ is predicted to increase quadratically in the missing momentum according to

$$\langle E_m \rangle = \frac{A-2}{A-1}\frac{p_m^2}{2M_N} + S_{2N} + \left\langle E_{A-2}^{hh'} \right\rangle \ , \tag{9}$$

where $S_{2N}$ is the threshold energy for two-nucleon knockout and $\left\langle E_{A-2}^{hh'} \right\rangle$ the average excitation energy of the $A-2$ system that was created after two nucleons escaped from the orbits characterized by the quantum numbers $h$ and $h'$. Moreover, the strength in the correlated part of the spectral function is often predicted to reside in a rather narrow region on both sides of $\langle E_m \rangle$ (the so-called "ridge" in the spectral function). For the sake of convenience, a panel with the exact location of the ridge in the $(E_m, \theta_p)$ plane was added to Fig. 4 and the contour plots corresponding with the upper and lower panels of Fig. 4 are shown in Fig. 5. Indeed, the major part of the calculated strength is concentrated in a wide band of missing energies about this ridge. Despite the fact that our calculations are unfactorized, the above observations with regard to the qualitative behavior of the calculated differential cross sections, illustrate that they exhibit the same qualitative features than what could be expected to happen in a factorized approach based upon the Eq. (7) using a realistic "correlated" spectral function.

Also the contribution of MEC and IC to the $^{16}$O$(e, e'p)$ reaction at high $E_m$

is shown in Fig. 4. For the kinematics considered there, they produce signals which are almost one order of magnitude larger than the combined effect of central and tensor correlations do. It is important to note that also the two-body currents create the major part of the $(e, e'p)$ strength along the ridge (Eq. (9)) in the $(E_m, \theta_p)$ plane. Therefore, the observation of a "ridge" should NOT always lead one to conclude that signatures of nucleon-nucleon correlations have been probed. Indeed, contaminations from two-body currents will feed similar parts of the $(e, e'p)$ phase space as the nucleon-nucleon correlations do. The MEC and IC effects are confined to the transverse part of the cross section, whereas the SRC mechanisms will feed both the longitudinal and transverse part. The observed transverse enhancement of the $^{12}$C$(e, e'p)$ cross section at high $E_m$ [17] can thus be naturally explained by the observations made in Fig. 4. The MEC and IC feeding of $A(e, e'p)$ at high $E_m$ will gradually lose in importance with increasing $Q^2$ and/or kinematic conditions corresponding with Bjorken x $\geq 1$ [16]. An example of what can be expected with more favorable kinematic conditions corresponding with Bjorken $x \approx 2$ is displayed in Fig. 6.

## 5 Conclusions

Signatures of nucleon-nucleon correlations (or, beyond mean-field behavior) are expected to reveal themselves in $A(e, e'p)$ at high missing energy and momentum and $A(e, e'NN)$. The $A(e, e'pp)$ data acquired over the past decade has indeed revealed evidence for short-range correlations, but indicated the importance of two-body currents as a highly competitive reaction mechanism. Tensor correlations are predicted to produce far stronger signals than the central short-range correlations and are presently under investigation with the $A(e, e'pn)$ reaction. Extracting clean information about the nuclear dynamics originating from nucleon-nucleon correlations requires the suppression of two-body current contributions. In $A(e, e'p)$ at high $E_m$ and $p_m$, such conditions can be accomplished at $Q^2$ values exceeding 1 GeV$^2$ and selective kinematics corresponding with Bjorken $x \approx 2$.

## References


[1] D.L. Groep *et al.*, Phys. Rev. C **63** (2001) 014005.
[2] R.A. Niyazov *et al.*, nucl-ex/0308013 and S. Gilad, contribution to this proceedings.
[3] K.I. Blomqvist *et al.*, Phys. Lett. **B421** (1998) 71.
[4] R. Starink *et al.*, Phys. Lett. **B474** (2000) 33.
[5] G. Rosner, Prog. Part. Nucl. Phys. **44** (2000) 99.
[6] D.P. Watts *et al.*, Phys. Rev. C **62** (2000) 014616.
[7] Niels R. Walet and R.F. Bishop, physics/0307069.
[8] D.O. Riska, Nucl. Phys. **A606** (1996) 251.
[9] Jan Ryckebusch, Phys. Lett. **B383** (1996) 1.

[10] C. Giusti, F.D. Pacati, K. Allaart, W.J.W. Geurts, W.H. Dickhoff and H. Müther, Phys. Rev. C **57** (1998) 1691.
[11] Marta Anguiano, Giampaolo Có and Antonio M. Lallena, J. Phys. G **29** (2003) 1119.
[12] J. Ryckebusch, M. Vanderhaeghen, L. Machenil and M. Waroquier, Nucl. Phys. **A568** (1994) 828.
[13] Marco Kahrau, Ph.D. thesis "Untersuchung von Nukleon-Nukleon Korrelationen mit Hilfe der Reaktion $^{16}\mathrm{O}(e,e'pp)^{14}\mathrm{C}$ in super-paralleler Kinematik", (Johannes Gutenberg-Universität, Mainz, 1999). URL : http://wwwa1.kph.uni-mainz.de/A1/publications/doctor/kahrau.ps.gz
[14] J. Ryckebusch and W. Van Nespen, nucl-th/0312056.
[15] D. Rohe, Eur. Phys. J. A **17** (2003) 439 and contribution to this proceedings.
[16] Stijn Janssen, Jan Ryckebusch, Wim Van Nespen and Dimitri Debruyne Nucl. Phys. **A672** (2000) 285.
[17] D. Dutta *et al.*, Phys. Rev. C **61** (2000) 061602.